Designer Descemet Membranes Containing PDLLA and Functionalized Gelatins as Corneal Endothelial Scaffold

Jasper Van Hoorick, Jasper Delaey, Hendrik Vercammen, Jürgen Van Erps, Hugo Thienpont, Peter Dubruel, Nadia Zakaria, Carina Koppen, Sandra Van Vlierberghe, and Bert Van den Bogerd*

Corneal blindness is the fourth leading cause of visual impairment. Of specific interest is blindness due to a dysfunctional corneal endothelium which can only be treated by transplanting healthy tissue from a deceased donor. Unfortunately, corneal supply does not meet the demand with only one donor for every 70 patients. Therefore, there is a huge interest in tissue engineering of grafts consisting of an ultra-thin scaffold seeded with cultured endothelial cells. The present research describes the fabrication of such artificial Descemet membranes based on the combination of a biodegradable amorphous polyester (poly (D,L-lactic acid)) and crosslinkable gelatins. Four different crosslinkable gelatin derivatives are compared in terms of processing, membrane quality, and function, as well as biological performance in the presence of corneal endothelial cells. The membranes are fabricated through multi-step spincoating, including a sacrificial layer to allow for straightforward membrane detachment after production. As a consequence, ultrathin (<1 µm), highly transparent (>90%), semi-permeable membranes could be obtained with high biological potential. The membranes supported the characteristic morphology and correct phenotype of corneal endothelial cells while exhibiting similar proliferation rates as the positive control. As a consequence, the proposed membranes prove to be a promising synthetic alternative to donor tissue.

1. Introduction

The cornea is the clear membrane that provides the eye a window to the exterior world. Several diseases or trauma can lead to an opaque cornea resulting in impaired vision and eventually blindness.[1,2] Many can only be treated with (partial) corneal transplantation, which is performed around 200 000 per year according to the most recent sources. Of that amount, around 40% are performed to cure corneal endothelial blindness.[3,4]

These patients suffer from an oedematous cornea due to a dysfunctional corneal endothelium, which is a monolayer of hexagonally shaped cells that covers the posterior corneal surface.[5] This cell layer is principally responsible for maintaining the cornea in a physiological state of deturgescence, which is imperative for its transparency. Corneal endothelial cells are incapable to undergo in vivo regeneration, meaning that the absolute number of cells will only decrease throughout life which can be further exacerbated by disease or trauma. When corneal endothelial cell density falls under a threshold of 500 cells mm^{-2}, corneal edema ensues leading to opacification and irreversible visual impairment.[6]

Dr. J. Van Hoorick, J. Delaey, Prof. H. Thienpont, Prof. P. Dubruel, Prof. S. Van Vlierberghe
Polymer Chemistry & Biomaterials Group
Centre of Macromolecular Chemistry (CMaC)
Department of Organic and Macromolecular Chemistry
Ghent University
Ghent 9000, Belgium

Dr. J. Van Hoorick, Prof. J. Van Erps, Prof. H. Thienpont, Prof. S. Van Vlierberghe
Brussels Photonics
Department of Applied Physics and Photonics
Vrije Universiteit Brussel and Flanders Make
Brussels 1050, Belgium

H. Vercammen, Prof. N. Zakaria, Prof. C. Koppen, Dr. B. Van den Bogerd
Antwerp Research Group for Ocular Science (ARGOS)
Translational Neurosciences
Faculty of Medicine
University of Antwerp
Wilrijk 2610, Belgium
E-mail: Bert.vandenbogerd@uantwerpen.be

Prof. N. Zakaria, Prof. C. Koppen
Department of Ophthalmology
Antwerp University Hospital
Edegem 2650, Belgium

ADVANCED
SCIENCE NEWS

www.advancedsciencenews.com

ADVANCED
HEALTHCARE
MATERIALS

www.advhealthmat.de

Currently, the standard of care is to surgically strip the dysfunctional cell layer and its underlying Descemet basement membrane from the corneal stroma and replace this with a viable corneal endothelium of a cadaveric donor cornea, termed endothelial keratoplasty.[7] More specifically, in Descemet stripping automated endothelial keratoplasty (DSAEK) the graft consists of endothelial cells, the Descemet membrane and some residual stroma that is inserted using a specialized cannula after which it automatically unfolds in the anterior chamber. In Descemet membrane endothelial keratoplasty (DMEK), there is no residual stroma, resulting in a thinner graft that spontaneously forms a roll that is unscrolled with an air bubble by the surgeon.[6] Regardless of good visual outcomes and minimal surgery-related complications, there is a severe global donor shortage that limits the number of corneal (endothelial) transplantations. A recent survey estimates that, in general for corneal transplantation, only one in 70 people requiring a donor cornea can be treated.[8]

This unfortunate situation has incited researchers to develop a cell therapy, based on the *ex vivo* expansion of corneal endothelial cells from one donor cornea to provide multiple patients with an answer to their sight-threatening condition. Recently, Kinoshita et al. have treated the very first patients with an injection of a corneal endothelial cell suspension and reported good visual recovery up to 2 years later.[9] Nevertheless, currently, the most investigated strategy is to create composite grafts of cells seeded onto a scaffold enabling transplantation similar to the currently applied corneal endothelial grafts. Such cell carriers, however, must exhibit very specific properties, such as transparency, glucose permeability, cytocompatibility, and above all, they must maintain the correct endothelial cell phenotype.[10] To date, attempts have been made to find an ideal corneal endothelial scaffold, which range from biological and biosynthetic to fully synthetic membranes. However, no candidate scaffold has met all requirements yet, nor has one effectively entered the clinic.[11]

An attractive scaffolding material in this respect is gelatin, which is obtained via hydrolysis of collagen, the main constituent of the natural extracellular matrix (ECM), rendering it a promising material for tissue engineering.[12] Furthermore, it is inexpensive, non-immunogenic, considered safe by the Food and Drug Administration (FDA) and displays the ability to be processed in line with a variety of applications.[12,13] Furthermore, due to the breakdown of the tertiary collagen protein structure into gelatin, it contains RGD (arginine-glycine-aspartic acid) motifs that promote cell attachment, rendering it cytocompatible and cell-interactive.[14] Furthermore, gelatin exhibits physical gelation properties, resulting in the formation of a hydrogel below its gel temperature (i.e., 30–35 °C).[15] Since this temperature is below the physiological temperature, it is often chemically modified to introduce chemical crosslinks to stabilize the gel above this gel temperature.[12,15–17] In the past, gelatin has already been used for corneal endothelial tissue engineering as a functionalized scaffold to grow cells on or as a bio-adhesive gelatin disc for transplantation.[18,19]

In this paper, we envisaged a combination of modified gelatin and a biodegradable polyester (i.e., poly(D,L-lactic acid), PDLLA), to develop a biocompatible scaffold for corneal endothelial transplantation. On the one hand, modified and crosslinked gelatins provide an ideal, stabilized ECM mimic to introduce cytocompatibility and cell interactivity. On the other hand, an un-

derlying PDLLA polyester base should provide the transplant with mechanical strength, thereby enabling corneal endothelial transplantation.

2. Experimental Section

2.1. Reagents and Consumables

Gelatin type A and B, isolated by an acidic and alkaline process respectively, was kindly offered by Rousselot. Furthermore, 1,4-dithiothreitol (DTT) (≥97%), glucose assay kit, acetic acid 3-(trimethoxysilyl) propyl methacrylate (98%), methacrylic anhydride (94%), NaOH, tetrahydrofurane (THF), and 5-norbornene-2-carboxylic acid were bought from Sigma-Aldrich. The PURASORB PDL 20 (PDLLA) was obtained at Corbion Purac (DMF-21817). Irgacure 2959 was supplied by BASF. Anhydrous K_2HPO_4 and Na_2HPO_4 were purchased at Fisher Scientific and 1-ethyl-3-(3-(dimethylamino)propyl)carbodiimide (EDC), N-hydroxysuccinimide (NHS), and Toluene were acquired from Acros Organics. Dimethyl sulfoxide (DMSO) was obtained from Chemlab, deuterium oxide from Euriso-top, and 2-aminoethyl methacrylate hydrochloride (AEMA.HCl) was purchased from Polysciences . Finally, dialysis membranes spectra/por (MWCO 12.000–14.000 g mol^{-1}) were obtained from Polylab . All reagents were used as received unless stated otherwise.

2.2. Preparation of Gelatin B Derivatives

2.2.1. Methacrylation of the Primary Amines in Gelatin B

The methacrylation of gelatin B, with the aim of obtaining gel-MOD (also known as gel-MA), was performed as described earlier.[16] Briefly, 100 g gelatin type B (38.5 mmol amines) was dissolved in 1 L of phosphate buffer (pH 7.8) at 40 °C under continuous mechanical stirring. Next, either 1 (i.e., 5.736 mL, 38.5 mmol) or 2.5 equiv. (i.e., 14.34 mL, 96.25 mmol) methacrylic anhydride were added and allowed to react for 1 h to obtain a high and a low degree of substitution (DS). After 1 h, the reaction mixture was diluted with 1 L double distilled water (DDW) ($\rho =$ 18.2 MΩ cm) followed by dialysis against distilled water (MWCO 12 000−14 000 g mol^{-1}) during 24 h at 40 °C, with the water being changed five times. The pH of the solution was adjusted to ≈7.4 using a 5 M NaOH solution. Finally, the gel-MOD was isolated by freezing and lyophilization (Christ freeze-dryer alpha I-5). The degree of substitution (DS) was determined using ^{1}H-NMR spectroscopy using D_2O as solvent at elevated temperature (40 °C) as reported earlier resulting in derivatives with a DS of 63% or 95%, respectively.[20]

2.2.2. Methacrylation of the Carboxylic Acids Present in Gel-MOD

Gel-MOD-AEMA was prepared following a previously reported protocol.[21] Fully functionalized gel-MOD (DS 95%) (10 g, 10.980 mmol carboxylic acids) was dissolved in 300 mL of dry DMSO (obtained via vacuum distillation over CaH_2) at 50 °C

ADVANCED
SCIENCE NEWS

www.advancedsciencenews.com

ADVANCED
HEALTHCARE
MATERIALS

www.advhealthmat.de

under inert argon atmosphere. After complete dissolution, 1 equiv. of EDC (2.1 g; 10.980 mmol) and 1.5 equiv. NHS (1.895 g; 16.48 mmol) were added together with 50 mL dry DMSO. After 30 min, 1.5 equiv. 2-aminoethyl methacrylate hydrochloride (AEMA.HCl) (2.729 g, 16.47 mmol) was added together with 50 mL of dry DMSO after which the solution was shielded from light and stirred overnight at 50 °C. DMSO was removed by dialysis (MWCO 12 000–14 000 g mol^{-1}) at 40 °C during 24 h in distilled water followed by freezing and lyophilization. ^{1}H-NMR spectroscopy in deuterium oxide was performed at 40 °C to determine the degree of substitution according to a previously reported protocol.[21]

2.2.3. Introduction of Norbornene Functionalities onto Gelatin

Gelatin-norbornene (gel-NB) was synthesized following a previously reported protocol.[21] In brief, the carboxylic acid functionalities in 5-norbornene-2-carboxylic acid were converted into an activated succinimidyl ester via reaction with EDC and NHS during 25 h, using a 1.25 times excess of 5-norbornene-2-carboxylic acid (relative to the amount of EDC added) to prevent the presence of unreacted EDC molecules which can on the one hand result in the formation of zero-length crosslinks between the primary amines and the carboxylic acids present in gelatin.[22] On the other hand, it is of predominant importance that all the EDC is reacted primary to the addition to the gelatin, as the combination of a carbodiimide and an acid catalyst (5-norbornene-2-carboxylic acid) in DMSO could result in oxidation of the alcohols present in gelatin to their respective aldehyde or ketone following a Pfitzner–Mofatt-oxidation.[23] These aldehydes could also result in crosslinking of the gelatin via reaction with the primary amines of gelatin resulting in Schiff's base formation.[12] To this end, EDC and NHS were dissolved in a respective 1:1.5 ratio in dry DMSO under argon atmosphere. In a next step, the temperature was raised to 50 °C and gelatin type B was added to the reaction mixture resulting in 0.75 equiv. of norbornene succinimidyl ester relative to the primary amines present in gelatin (0.385 mmol g^{-1}) and allowed to react for another 20 h. Next, the mixture was precipitated in a tenfold excess of acetone, filtered on filter paper (VWR, pore size 12–15 µm) using a Büchner filter to remove the formed ureum side products and DMSO, followed by dissolving in DDW and dialysis for 24 h against distilled water (MWCO 12–14 kDa). After dialysis, the pH of the mixture was adjusted to ≈7.4 using a 5 M NaOH solution. Finally, the pure product was isolated by freezing and lyophilization. The DS was assessed using ^{1}H-NMR spectroscopy in D2O at 40 °C as previously reported.[21] The derivative exhibited a DS of 63%.

2.3. Polymer Characterization

2.3.1. Nuclear Magnetic Resonance Spectroscopy

The ^{1}H-NMR spectra of the gelatin derivatives were recorded at 40 °C using a 500 MHz Bruker Avance II Ascend spectrometer. All other ^{1}H-NMR spectra were recorded using a 400 MHz Bruker Avance II Ultrashield spectrometer at room temperature.

Analysis of the obtained spectra was performed using MestReNova software.

2.3.2. Photo-Rheology

Photo-rheological measurements were performed on an Anton–Paar Physica MCR 301 rheometer using a plate-plate geometry (upper plate diameter: 25 mm). All measurements were performed at 37 °C at an oscillation frequency of 1 Hz with a strain of 0.1% (selected based on the linear viscoelastic area as previously reported) and a gap setting of 0.35 mm.[16] Samples were trimmed, sealed with vacuum grease to prevent drying (Bayer silicone, mittelviskös, VWR) and irradiated through a quartz glass bottom plate using UV-A light at 365 nm and an intensity of 500 mW cm^{-2} (EXFO Novacure 2000 UV light source). Samples were irradiated with UV light for 10 min and were measured during this treatment and 2 min before and after. All applied samples were crosslinked at a 10 w/v% gelatin concentration in the presence of 2 mol% Irgacure 2959 as photoinitiator, relative to the number of crosslinkable functionalities. The norbornene derivative solutions also contained 0.5 equiv. DTT as a crosslinker corresponding to an equimolar thiol-ene ratio, allowing for efficient crosslinking.

2.3.3. Size Exclusion Chromatography

Size exclusion chromatography was performed on the PDLLA polyesters to determine the number average molecular weight (M_n), weight average molecular weight (M_w), and polydispersity index. The measurements were performed on a Waters Alliance 2695 set-up (Zellik, Belgium) coupled to an Agilent (Diegem, Belgium) guard column (PLGel 5 µm) and a mixed-D LS polystyrene-divinylbenzene (300 × 7.5 × 5 µm) column from Polymer Laboratories (Middelburg, The Netherlands). Detection was based on a Waters refractive index detector 2414. The molecular weights were determined from the obtained retention times via an external calibration curve using polystyrene standards (1.2–177 kg mol^{-1}). As eluent HPLC grade chloroform at a flow rate of 1 mL min^{-1} was applied.

Samples were prepared by dissolving 10 mg of polymer in 2 mL HPLC grade chloroform. The resulting solutions were passed through a 0.45 µm syringe filter, transferred to a mass vial, and subsequently analyzed. Furthermore, a correction factor of 0.58 was applied to the results to compensate for the difference in hydrodynamic volume between the polystyrene standards and the PDLLA.[24]

2.4. Membrane Production

Membranes were produced by a multistep spin coating process in the following order: i) gelatin A, ii) PDLLA, and iii) crosslinkable gelatin B derivatives, with the specific parameters mentioned in **Table 1**. The purasorb PDL 20 are PDLLA polymers regulated by the FDA and covered with a Device Master file (MAF 1961) and drug master file (DMF 31 084).[25,26] After the

ADVANCED
SCIENCE NEWS

www.advancedsciencenews.com

**ADVANCED
HEALTHCARE
MATERIALS**

www.advhealthmat.de

Table 1. Overview of the applied spincoating parameters during the membrane fabrication process.

#	Type		concentration	Spincoating Parameter (Acceleration in RPM S^{-2}) Speed [RPM]	Photoinitiator	Crosslinker	Volume 12 mm ø	Volume 25 mm ø
1	Gelatin A		10 w/v% (in DDW)	750 RPM s^{-2} (2000 RPM for 60 s)	/	/	60 µL	250 µL
2	PDLLA		4 w/w% (in THF)	1000 RPM s^{-2} (3000 RPM for 60 s)	/	/		
3	Gelatin B	gel-MOD	10 w/v% (in PBS)	750 RPM s^{-2} (2000 RPM for 60 s)	Irgacure 2969 2 mol%	/		
		Gel-MOD-AEMA	10 w/v% (in PBS)			/		
		Gel-NB	10 w/v% (in PBS)			DTT (1 to 1 thiol/ene ratio)		

PDLLA layer was deposited, the samples were subjected to a 0.8 mbar Argon plasma treatment for 30 s with a Diener electronic plasma treatment device to enable a better compatibility and co-valent attachment of the gelatin derivatives to the PDLLA after crosslinking.[27,28] Finally, crosslinking of the gelatin B derivatives was performed by hydrating the coated gelatin layer with 60 or 250 µL of DDW (for samples with a diameter of 12 and 25 mm respectively) and irradiating the samples for 10 min from top and bottom with UV-A light at a wavelength of 365 nm with an intensity of 4 mW cm^{-2} using a high performance ultraviolet transilluminator (ultra violet products).

2.5. Membrane Characterization

X-ray photoelectron spectroscopy (XPS) measurements were performed on four random locations of the measured samples in duplo for elemental analysis of the spin coated layers. An ESCA S-probe VG monochromatic spectrometer with an Al Kα X-ray source (1486 eV) was used to measure a spot size of 250 µm by 1000 µm, which was analyzed using the Casa XPS software package.

Static contact angles of the produced membranes were determined, hereby measurements were conducted on membranes attached to methacrylated glass slides without the presence of a sacrificial gelatin layer since no membrane detachment was desired. Measurements were conducted using an OCA 20 device using the software provided by the supplier (i.e., SCA 20, version 2.1.5 build 16). A 1 µL droplet of DDW was used to determine the contact angles. The contact angle for each sample was determined as the average during the first 30 s. All measurements were performed in triplicate.

Transparency of the membranes coated on glass-plates was measured using a custom made set up consisting of a broadband halogen light source (Avantes Avalight–Hal) which was guided toward the sample holder using an optical fiber. The transmitted light was transferred to a broadband spectrum analyzer (Avantes Avaspec—2048). In this way transmission at all wavelengths was measured simultaneously after performing a baseline correction. Furthermore, during the measurement the sample holder was covered with a black case to remove influence of stray light. Transmission of all coated glass slides was compared relative to a glass slide with a gelatin A coating. For the hydrated samples, a droplet of deionized water (300 µL) was placed on each sample, and they were allowed to reach equilibrium swelling during 90 min prior to the measurement.

Finally, the thickness of the membranes was determined with the use of a BRUKER Contour GT-I white light interferometric 3D surface metrology optical microscope. Samples were scratched with metal forceps to expose the multiple layers. The thickness was then measured from the glass to the top of the coating using depth profilometry. (see Figure S1, Supporting Information).

Mechanical analysis was performed on PDLLA basement membranes. To this end, large samples ($d = 25$ mm) were detached from the glass slide by dissolving the sacrificial gelatin layer. Next, they were placed in between two pieces of paper and cut in ribbons of ≈7–8 mm wide. Next, these ribbons were placed in a tensile testing device followed by removal of the paper (Lloyd TA500 Texture Analyser, equipped with a 10 N load cell) and the exact width and gauge length of the sample were measured using digital calipers. The thickness of the samples was selected as the average from the optical profilometry measurements (see Figure 4E). The samples were stretched at a speed of 5 mm min^{-1} while monitoring the load (in N). From this data, stress-strain plots were generated where the strain (%) is obtained by dividing the elongation by the gauge length, whereas the stress (MPa) is obtained by dividing the measured load by the surface area of the sample (width × thickness). The Young's modulus was calculated from the slope of the linear part of the stress-strain curves. All experiments were performed in triplicate.

Glucose diffusion was evaluated by placing a membrane in a side-by-side diffusion set up. To this end, a 10 w/v% glucose solution in double distilled water was prepared with 0.5 w/v% sodium azide added to prevent growth of micro-organisms. The setup is built up out of two diffusion cells, each diffusion cell is supplied with a stirring bar and kept at a constant 37 °C. The produced membranes were clamped between the diffusion cells. One of the two diffusion cells is filled with 2.5 mL of the previously prepared glucose solution, termed the donor cell. The other diffusion cell is filled with 2.5 mL of double distilled water, which is the acceptor cell. The acceptor cell is periodically emptied inside a mass tube and then refilled with 2.5 mL double distilled water. The collected fractions of the acceptor cell are then diluted

100 times and analyzed using a glucose oxidase assay. The apparent permeability constant (P_{app}) was calculated according to the following equation.[31]

$$P_{app} = \frac{\frac{dC}{dt}}{(A \times C_0)} \tag{1}$$

Where $\frac{dC}{dt}$ is the change in concentration over time as determined by the linear regression of the measurements at different time points (mol s^{-1}).

A is the exposed surface of the membrane (cm²) (i.e., 0.79 cm²).

C_0 is the initial glucose concentration (mol cm^{-3}) (i.e., 0.55×10^{-3} mol cm^{-3}).

2.6. Biological Assays

Glass coverslips coated with the gelatin B derivatives were used in order to test the interaction between gelatin and endothelial cells without the sacrificial gelatin A layer or the PDLLA. The glass coverslips were first methacrylated to ensure covalent attachment between the gelatin derivatives and the glass coverslips.

To this end, they were cleaned with DDW, acetone, and subjected to a 3-min argon plasma treatment. Following this, they were incubated in a mixture containing 50 mL DDW, 48 mL ethanol, 0.3 mL acetic acid, and 2 mL 3-(trimethoxysilyl) propyl methacrylate for 30 min followed by thorough rinsing with DDW.

In brief, the spincoated samples on glass coverslips (diameter 12 mm) were secured into a 24 well tissue culture plate using the cellcrown insert (Scaffdex, Tampere, Finland).

To sterilize the samples, they were incubated in a range from 30–70% ethanol solution with a 10% increment every 30 min. They were stored overnight in a 70% solution, and irradiated with UV-C for 30 min. Next, they were rinsed with sterile PBS (3X) and exposed to UV-C irradiation for another 30 min prior to use.

2.6.1. Cell Culture

B4G12 immortalized corneal endothelial cells (DSMZ, Braunschweig, Germany) were cultured according to the manufacturer's instructions with minor modifications. In brief, the cells were grown on tissue culture treated plastic ware, coated with an FNC coating mix (Athena Enzyme systems, Baltimore, USA). The growth medium consisted of human endothelial serum free medium (Life Technologies) supplemented with 10 ng mL^{-1} basic fibroblast growth factor (Life Technologies) without antibiotics. B4G12 cells were detached using 0.05% Trypsin-EDTA (Life Technologies) and subcultured or seeded according to the downstream assay.

2.6.2. Immunocytochemistry

Corneal endothelial cells were cultured on glass coverslips coated with gel-MOD-AEMA, gel-MOD DS63, gel-MOD DS95, gel-NB DS63. After 7 days in culture, the samples were fixated in ice cold paraformaldehyde 4% for 30 min, rinsed three times in PBS

1X (Life Technologies) and stained within 1 week. The samples were permeabilized with PBS1X containing 1% Triton X-100 for 30 min and incubated overnight with a primary antibody raised against ZO-1 (1:200; Thermo Fisher Scientific, Massachusetts, USA) or Na$^+$/K$^+$ ATPase (1:40; Santa Cruz Biotechnology, Texas, USA) for phenotyping. The secondary antibody (goat anti-mouse FITC 1:500; Jackson Immunoresearch, West Grove, USA) was incubated for 2 h at room temperature in the dark, followed by a nuclear stain with 100 µg mL^{-1} 4′,6-diamidino-2-phenylindole (DAPI) (Sigma, St. Louis, USA) and mounted using Citifluor to reduce fading (Citifluor, Hatfield, USA). Images were captured using an UltraView VOX laser spinning disk confocal microscope (Perkin Elmer, Massachusetts, USA) at 20× magnification and processed using ImageJ.

For the adhesion assay, samples seeded with 25 000 cells for 24 h were subjected to a similar protocol with primary anti-vinculin antibodies (1:200, Abcam, Cambridge, United Kingdom) and secondary goat anti-mouse PE conjugated antibodies. Images were processed according to a previous published protocol.[10] Both primary and secondary antibodies were diluted in 0.01 M PBS containing 0.5% Thimerosal, 0.1% NaN$_3$, 10% normal horse serum, and 0.3% bovine serum albumin.

2.6.3. Proliferation Assay

A proliferation assay was performed in the Incucyte (Sartorius, Göttingen, Germany), a high-throughput live-cell imaging system. B4G12 cells were seeded with a density of 30 000 cells per well and incubated for 4 h (37 °C, 5% CO2) until adherent. Next, the nuclei were counterstained with NucLight Rapid Red Reagent 1:2000 (Sartorius, Göttingen, Germany) and imaged every 2 h (see Video S1, Supporting Information). Using the built-in software, custom masking algorithms were generated to quantify cellular growth expressed as #nuclei mm^{-2} as a function of time. Growth curves were fitted using Graphpad Prism 8.0 using an exponential growth fitting curve model and population doubling times (PDT) were extracted. PDT were then statistically compared to each other using a non-parametric Kruskal–Wallis test where $p < 0.05$ was deemed significant.

2.6.4. Primary Corneal Endothelial Cell Culture

Primary corneal endothelial cells were isolated and cultivated according to previous reports using a peel-and-digest method.[10,32] The donor corneas used for this research were excluded from transplantation and made available for research. Ethical approval was granted by the local ethical committee (EC14/30/319). First, the endothelium and Descemet membrane were mechanically dissected from the posterior cornea using micro-forceps and an operating microscope. Second, the harvest tissue was further digested in a 1 mg mL^{-1} collagenase 1A (Sigma Aldrich, St. Louis, USA) for 2 h at 37 °C and 5% CO$_2$. Dislodged cells were further digested using trypLE Express Enzyme (Thermo Fisher Scientific, Massachusetts, USA) for 5 min at 37 °C. Finally, cells were pelleted at $72 \times g$ for 5 min and seeded in an FNC coated 24 well plate. Two donor corneas of the same donor were

ADVANCED
SCIENCE NEWS

www.advancedsciencenews.com

ADVANCED
HEALTHCARE
MATERIALS

www.advhealthmat.de

pooled and cells were cultivated for 7 days before performing immunocytochemistry for ZO-1 and Na$^+$/K$^+$ ATPase as described earlier.

2.7. Statistics

Statistical significance was analyzed using GraphPad Instat using a one-way analysis of variance (ANOVA) with bonferroni post-test in case of a normal distribution and adequate sample size. Non-parametric Kruskal-Wallis was applied in case of a lower sample. Statistical significance was defined as *** $p < 0.001$, ** $p < 0.01$, * $p < 0.05$.

3. Results and Discussion

3.1. Material Development and Characterization

In order to obtain a stable gelatin coating at 37 °C, the material needs to be chemically crosslinked to circumvent the physical dissociation behavior at 30 °C of unmodified gelatins.[15] Therefore, the present work explores the use of different chemically modified photo-crosslinkable gelatins including gel-MOD, gel-MOD-AEMA, and gel-NB.[12,15,16] In this respect, gel-MOD and gel-MOD-AEMA are crosslinked following a free radical chain growth polymerization mechanism, whereas gel-NB is crosslinked using a thiol-ene step growth polymerization mechanism using DTT as thiolated crosslinker. Additionally, derivatives with a different number of crosslinkable groups were compared. The first and most common derivative, gel-MOD, was used with two different degrees of amine substitution, namely 63% and 95% (corresponding to 0.243 and 0.367 mmol g^{-1} gelatin respectively). These derivatives were obtained via the reaction of the primary amines present in the (hydroxy)lysine and ornithine amino acids with 1 or 2.5 equiv. of methacrylic anhydride respectively (**Figure 1**; top panel).[16]
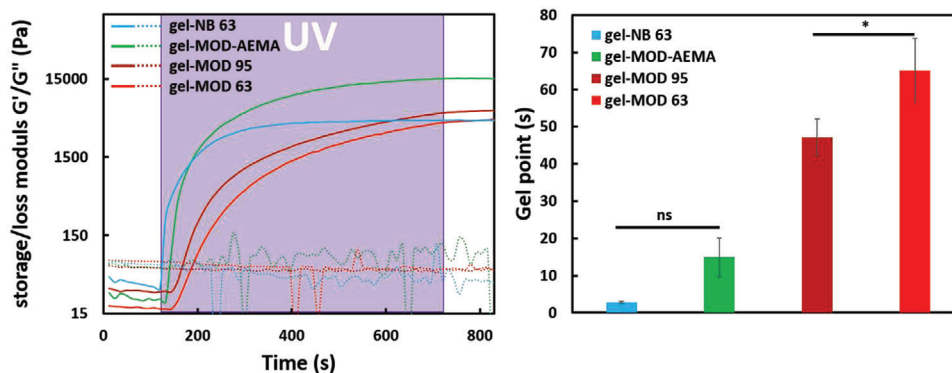
Apart from gel-MOD, gel-MOD-AEMA was also assessed, which is another derivative containing more crosslinkable functionalities.[15] This derivative is obtained starting from gel-MOD with a high degree of substitution (i.e., DS 95) via subsequent reaction of the carboxylic acids present in the side chains of the glutamic acid and aspartic acid amino acids with 2-aminoethyl methacrylate hydrochloride (AEMA) using carbodiimide coupling chemistry (EDC/NHS). As a result, a DS for the carboxylic acids of 55% was obtained, corresponding to 0.6039 mmol methacrylates per g gel-MOD-AEMA. When combining the latter value with the 0.367 mmol methacrylamides per g resulting from the amine substitution, a total of 0.97 mmol crosslinkable groups per g gel-MOD-AEMA was obtained (see Figure 1, middle panel).[15]

A third crosslinkable gelatin derivative (gel-NB) applies thiol-ene photo-click chemistry to generate a crosslinked network. For this derivative, the primary amines of gelatin were functionalized with 5-norbornene-2-succinimidyl ester, yielding gel-NB with a DS of 63%, corresponding to 0.243 mmol g^{-1} gel-NB (Figure 1, bottom panel).[21]

To compare the different reactivities of the applied derivatives, photo-rheological measurements were performed on 10 w/v% solutions in the presence of 2 mol% (in respect to the amount of incorporated crosslinkable functionalities) Irgacure 2959 as photoinitiator, and 0.5 equiv. of DTT (i.e a 1:1 thiol:ene ratio) for the norbornene derivative. Irgacure 2959 was selected as photoinitiator, due to its known biocompatible behavior.[31] The assay provides insight in the reactivity of the materials as well as the mechanical properties of the gelatin coatings after crosslinking. In accordance to previous research, the material with the highest density of crosslinkable functionalities (gel-MOD-AEMA) resulted in the highest stiffness as reflected by the storage modulus (G') after 10 min of crosslinking.[15] This derivative reached a storage modulus of around 15 kPa whereas gel-MOD DS95 reached a storage modulus of around 6 kPa. The gel-MOD DS63 and gel-NB DS63 derivatives yielded storage moduli around 4.5 kPa (**Figure 2**; right panel). When Palchesko et al. investigated the influence of mechanical properties on the expansion behavior of bovine corneal endothelial cells, they observed the optimal
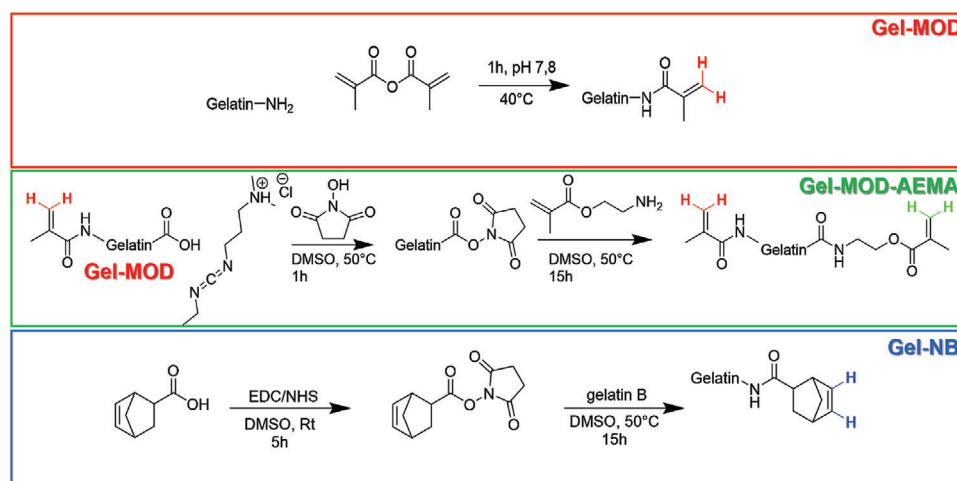
Figure 1. Applied gelatin modification strategies via the introduction of methacrylamides (red) yielding gel-MOD; the subsequent introduction of methacrylates into gel-MOD yielding gel-MOD-AEMA (green), and the introduction of norbornene functionalities (blue) yielding gel-NB.

**ADVANCED
SCIENCE NEWS**

www.advancedsciencenews.com

**ADVANCED
HEALTHCARE
MATERIALS**

www.advhealthmat.de

Figure 2. Photo-rheological monitoring of crosslinking kinetics and resulting mechanical properties at 37 °C with the evolution of the storage moduli (G') depicted as solid lines, whereas the loss modulus (G'') is depicted using dashed lines. (Left panel); Average gel-points (in seconds) after switching on the UV light for the different crosslinking systems as a measure of crosslinking reactivity ($n = 3$) (Right panel). All differences were significant with $p < 0.001$ except for the ones indicated in the picture with * ($p < 0.05$) or ns (not significant).

mechanical properties being around a Young's modulus (E') of 50 kPa, which resembles the microscopic Young's modulus of the Descemet membrane (i.e., as perceived by the cells).[33,34] To put this in perspective, we made an estimation for the Young's modulus (E') following Equation (2).[35]

$$E' = 2G'(1 + \mu) \tag{2}$$

Here, μ is the Poisson number which equals 0.5 for ideal rubbery materials, which is a good approximation for hydrogels.[35,36] As a consequence, the gel-MOD-AEMA derivative reaches a Young's modulus of around 45 kPa, while the high DS gel-MOD reach Young's moduli around 18 kPa and the low DS gel-MOD and the gel-NB derivatives around 13.5 kPa. As a consequence, the gel-MOD-AEMA should provide the closest match to the reported optimal Young's Modulus of 50 kPa.[33,34]
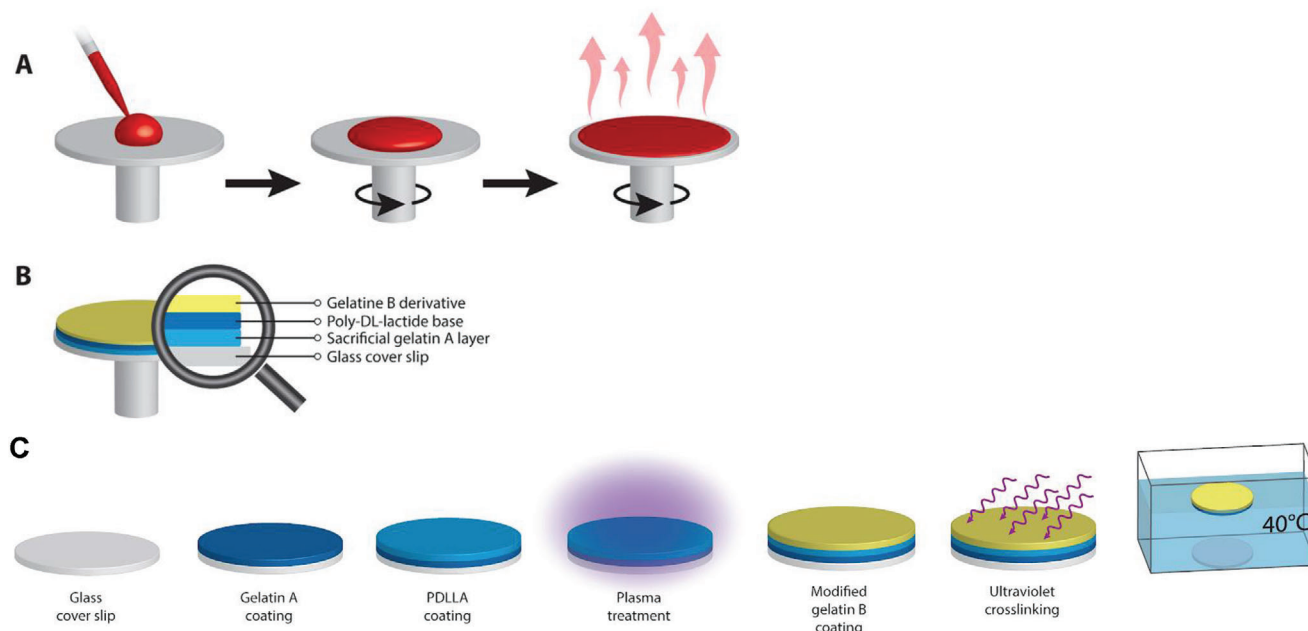
We compared the gel points of the different materials as an indication of reactivity thereby providing information about the minimally required irradiation time. Here, the drastic increase in reactivity for norbornene derivatives over the more conventional systems is apparent (Figure 2; right panel). The norbornene derivative has a gel point in the range of a few seconds (i.e., 2–3) versus > 50 s for the gel-MOD derivatives, with the gel-MOD-AEMA derivative being intermediate, at ≈15 s (see Figure 2; right panel). The faster crosslinking kinetics are the consequence of different aspects. First, the norbornene systems are crosslinked using a thiolated crosslinker (DTT) following thiol-ene photo-click chemistry which is not prone to oxygen inhibition and therefore not associated with a lag time after switching on the UV light during which residual oxygen would need to be consumed prior to initiation.[37,38] Second, especially thiol-ene reactions exploiting norbornene functionalities as "-ene" moiety are characterized by a very high reactivity due to the ring strain relief and the rapid subsequent hydrogen-abstraction of a thiol hydrogen by the carbon-centered radical.[39] Additionally, the increased reactivity of gel-MOD-AEMA over conventional gel-MOD is the consequence of two other factors. First, methacrylates exhibit a higher reactivity in comparison to the methacrylamides present in gel-MOD. Second, the photoinitiator is added in a 2 mol% ratio relative to the number of crosslinkable groups present. Since gel-

MOD-AEMA has roughly three times more crosslinkable groups, likewise three times more radicals will be formed at the same time in the gel-MOD-AEMA solution upon irradiation resulting in higher degrees of initiation culminating in a faster increase in mechanical properties. However, this also increases the probability of termination which can hamper the reactivity. On the other hand, due to the presence of more crosslinkable functionalities, the probability of termination will again be lower as the formed radicals will have a higher chance to encounter unpolymerized methacryloyl functionalities rather than recombining with another radical.

Furthermore, although the introduction of crosslinks in the gelatin derivatives result in stability at physiological conditions, the reported gelatin derivatives still exhibit their favorable enzymatic biodegradability as previously reported for gel-MOD, gel-MOD-AEMA, and gel-NB.[15,40]

3.2. Membrane Production

To obtain ultrathin membranes (i.e., the natural Descemet membrane exhibits thicknesses around 10–12 μm[30]), a multi-step spin coating approach was applied. First, a layer of unmodified gelatin A was applied on a supporting glass substrate, as sacrificial layer to enable dissolution in a final step after incubation in water at 40 °C to enable membrane harvesting (see Video S3, Supporting Information). Next, a polyester base membrane was applied through spin coating, starting from a solution of PDLLA in THF. To this end an amorphous poly(D,L-lactide) of 150 kg mol^{-1} and a polydispersity of 1.13 was chosen for several reasons. First of all, PDLLA is an FDA-approved generally recognized as safe polymer for use in the human body with many applications in drug products and multiple FDA medical device approvals including the use as dermal fillers or bioresorbable vascular stents.[41–43] Second, PDLLA was chosen over the more conventional PLLA as PDLLA is an amorphous material which results in a high transparency.[44] Finally, PDLLA is a biodegradable material resulting in non-toxic lactic acid based degradation products as previously reported.[45] This is a specific benefit toward corneal endothelial repair as in vivo 85% of the glucose

**ADVANCED
SCIENCE NEWS**

www.advancedsciencenews.com

**ADVANCED
HEALTHCARE
MATERIALS**

www.advhealthmat.de

Figure 3. A) The principle of spin coating. B) The final composition of the obtained membranes. C) Scheme of the multistep spin coating approach to produce the membranes.

nutrients which enter the cornea is metabolized to lactic acid, which diffuses back through the corneal endothelium. As a consequence, the tissue is characterized by relatively high lactic acid concentrations (i.e., 13 mm in the cornea and 7 mm in the anterior chamber).[46] Therefore, it is anticipated that PDLLA is an ideal scaffolding material, as the degradation products will not induce any inflammation and the lactate is even considered as a contributing anion flux to maintain corneal transparency.[46] To allow covalent adhesion between the polyester and the subsequent crosslinkable gelatin layer, the surface was activated using a plasma treatment.[28] Finally, the crosslinkable gelatin solution was applied starting from a solution containing 2 mol% Irgacure 2959, and an equimolar amount of thiols (DTT) with respect to the NB functionalities for the gel-NB derivative.[21] Gelatin was chosen as an extra cellular matrix mimic due to the structural similarities with collagen, the main component of the natural Descemet membrane.[22,47] Furthermore, the material is known to be biodegradable resulting in the formation of peptides in vivo, similarly to collagen breakdown in the human body.[12,15,48] Crosslinking and covalent attachment of this gelatin layer occurred by UV irradiation after prewetting of the surface with double distilled water.[27] Finally, the membranes were detached by immersion in water above the gel temperature of gelatin (i.e., ± 30 °C) (**Figure 3**C and Video S2, Supporting Information).[15] In respect of membrane fabrication, it should be noted that the gel-MOD-AEMA derivative exhibits a benefit over the other reported derivatives, as the high degree of modification hampers triple helix formation resulting in solubility at room temperature.[15,22,49] As a consequence, material manipulation during spin coating becomes more straightforward (i.e., a more homogeneous deposition) as there are no issues with premature gel formation.

3.3. Membrane Characterization

XPS elemental surface characterization was performed after each of the aforementioned steps in the multi-step spin coating process to validate the successful application of the respective layers. The results show that the elemental composition of the surface differed after each step. There was an anticipated high silicium level (i.e., ±20%) from the glass substrate and nitrogen signal in the (modified) gelatin layers (i.e., ±4% to ±16%)(**Figure 4**A) as a consequence of the peptide backbone and the nitrogen atoms present in the side chains of the (hydroxy)lysine, ornithine, histidine, proline, and arginine amino acids present in gelatin. Additionally, the N/C ratio diminished with increasing degree of substitution for the gelatin derivatives since more carbons are attached per amine (i.e., from ±0.18 to ±0.05). Especially for gel-MOD-AEMA, this ratio drastically decreased since the introduced AEMA functionalities have a very high C/N ratio (i.e., 6/1). Furthermore, when looking at the O/C ratio of the PDLLA membrane, this corresponds to 0.67 thereby proving that indeed the surface was covered with PDLLA since every repeating unit in the polymer chain contains three carbon atoms and two oxygen atoms.

Further proof of a successful coating process could be found by measuring the static contact angle of water on the different substrates (Figure 4B). After initial coating of the glass with PDLLA, the contact angle increased (i.e., from 69° to 81°) due to the relatively hydrophobic nature of PDLLA. After plasma treatment, reactive oxygen containing functional groups are introduced at the surface, which leads to an increased hydrophilicity as evidenced by a decreased contact angle (i.e., 55°).[27,51] Subsequent coating with the gelatin derivatives reduces this hydrophilicity. However, when comparing the non-plasma treated
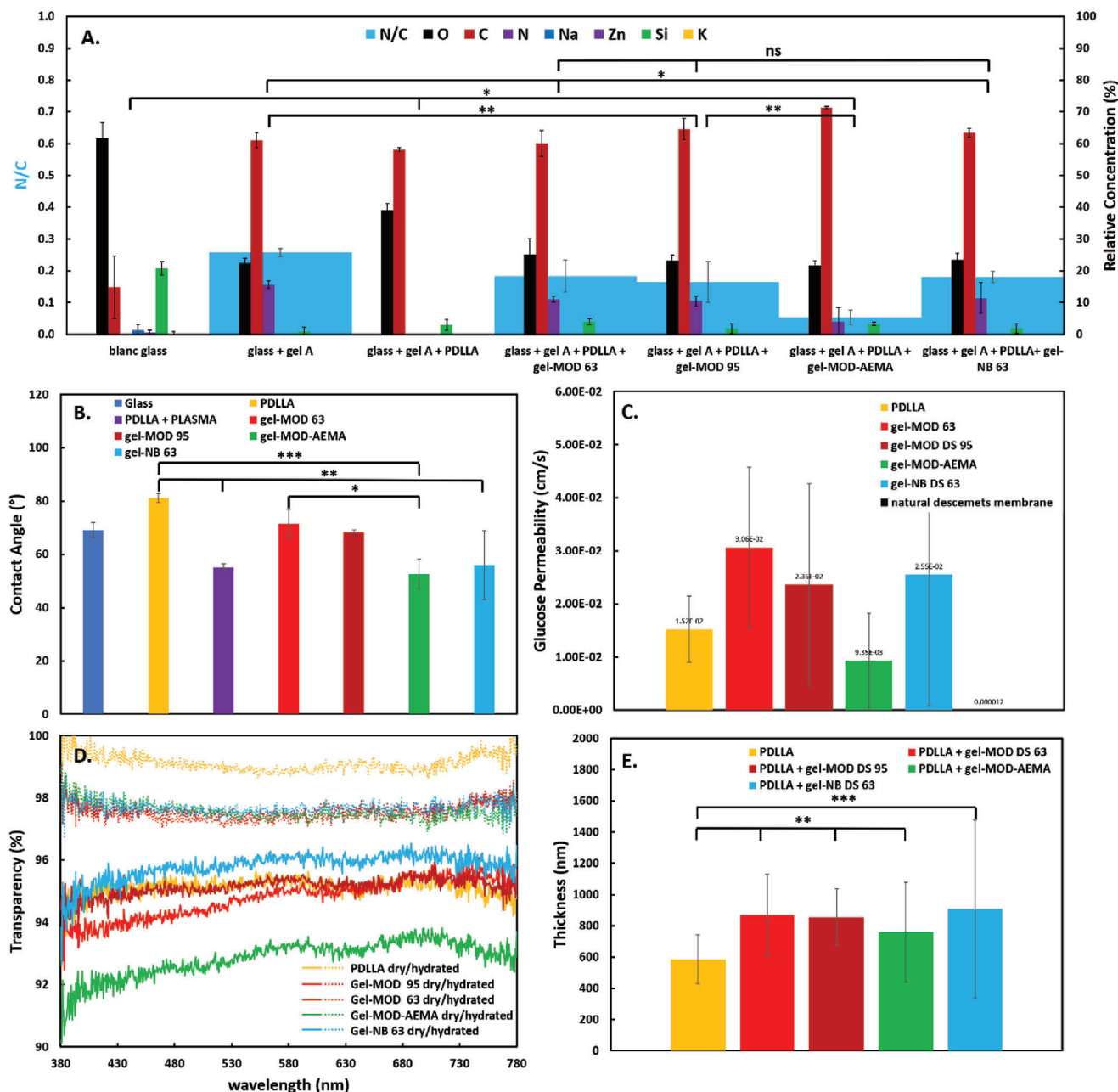
Figure 4. A) X-ray photoelectron spectroscopy elemental analysis of the top layer of the membrane during stepwise membrane production. B) Static contact angle measurements indicating hydrophilicity on the different membranes. C) Glucose permeability of the different membranes relative to the natural Descemet membrane.[50] D) Transparency of the different membranes throughout the visual spectrum both in the dry (solid lines) and in the hydrated state (dashed lines) (n = 4). E) Membrane thickness measurements, as determined using optical profilometry. (All statistical differences are denoted with * for p < 0.05, ** for p < 0.01 and *** for p < 0.001 with the exception of panel (A) where all differences are p < 0.001 unless denoted otherwise (with "ns" representing no statistical significance).

PDLLA with the gelatin coatings, a significant difference can be observed, thereby again confirming successful membrane functionalization. Although some differences between the different gelatin coatings appear present, these are non-significant with the exception between gel-MOD DS 63 and gel-MOD-AEMA where gel-MOD-AEMA is significantly more hydrophilic (p < 0.05).

3.4. Membrane Function

One of the predominant requirements of an artificial Descemet membrane is that it should be sufficiently transparent in the visual range (i.e., ≥90% for the natural Descemet membrane[10]), not to impair the vision of the patient after transplantation.[11] When assessing the transparency of the produced membranes
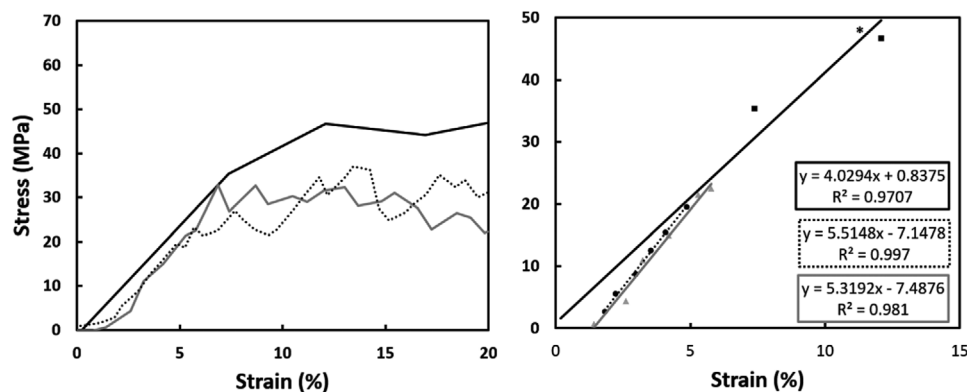
Figure 5. Stress–strain plot of the PDLLA membranes obtained via tensile tests (left panel). Zoom of the linear region and calculated Young's moduli as determined by the slope (right panel).

qualitatively, it seems that throughout the different production steps, the membranes exhibited comparable transparency in reference to the glass slide on which they were coated, since the underlying pattern can clearly be distinguished (Figure 6). Additionally, after isolation from the supporting glass slide by dissolution of the sacrificial gelatin layer (Figure 6H), the membranes exhibited sufficient mechanical integrity to allow for surgical manipulation (see Videos S2 and S3, Supporting Information). It should be noted that in contrast to natural donor endothelium, the currently reported membranes did not exhibit the same self-scrolling behavior of a DMEK graft. However, it is anticipated, that the scaffold could be introduced by using a suitable surgical tool to introduce it into a cannula similar to a DSAEK procedure.[19]

As a proof of concept experiment toward surgical manipulation, the membranes could be mounted into cell crowns without rupturing (Figure 6K,L). To quantify the mechanical integrity of the developed membranes, they were subjected to tensile tests to determine the Young's moduli. In this respect, only the mechanical properties of the base PDLLA membranes were measured in the absence of the gelatin coating. This was done deliberately, as the gelatin coating, a soft hydrogel with a Young's modulus in the range of a few kPa (vide supra) which will have a negligible effect in comparison to PDLLA which is a robust polyester. Indeed, the tensile tests indicated that the PDLLA membranes are characterized by a Young's modulus of 4.95 ± 0.81 MPa, which is two orders of magnitude higher than the calculated Young's moduli for the gelatin hydrogels (**Figure 5**). These mechanical properties further demonstrate the suitability of the developed membranes as corneal endothelial scaffolds, as literature states that the natural Descemet membrane is characterized by a comparable macroscopic Young's modulus (i.e., 2.5–5 MPa).[50,52] Since similar mechanical properties are obtained in comparison to the natural Descemet membrane, the membranes should also allow surgical manipulation using conventional surgical techniques applied for the transplantation of natural Descemet membranes.

Additionally, also after membrane isolation, still sufficient transparency was observed (i.e., PDLLA + gel-MOD-AEMA in **Figure 6I,J**). Although, it should be noted that transparency was somewhat compromised in the dry state (Figure 6I) due to wrinkling of the membrane. However, after rehydration, (Figure 6J) the underlying pattern becomes very clear again, indicating

sufficient transparency. Quantitative spectrophotometric measurements indicated that all membranes exhibited over 90% transparency in the visual spectrum in the dry state with gel-MOD-AEMA being the least transparent (i.e., 90–94%) while still exhibiting a comparable transparency to the natural Descemet membrane.[10] (Figure 6D) In addition, the transparency of the membranes was also assessed on hydrated samples to provide a better mimic of the natural tissue. being more representative for in vivo conditions. After hydration, the transparency of the gelatin-coated materials increased to >97% for all membranes with no significant differences in transparency whereas the uncoated PDLLA membrane exhibited transparencies around 100% throughout the spectrum however also not significantly higher in comparison to the gelatin coated membranes. Since the natural Descemet membrane is characterized by 90% transparency in the visual spectrum, these membranes proof to be suitable as a natural Descemet membrane substitute with respect to optical characteristics.[10]

Additionally, the thickness of all membranes (i.e., <1 µm) was below the thickness of the natural Descemet membrane (i.e., 10–12 µm) thereby qualifying as a proper surrogate Descemet membrane in terms of dimensions (Figure 4E). Other gelatin-based hydrogels that have been reported earlier for corneal endothelial tissue engineering are either crosslinked with toxic reagents[53] or are thicker.[18,19,54] Thick constructs would eventually lead to loss of visual acuity in patients.[10,30,55] Furthermore, experiments indicate that one way to tune the thickness of the membranes without affecting the transparency is to apply multiple coatings on top of each other rather than changing the concentration of the polymer in the spin coating solution (see Figure S2, Supporting Information).

The most important function of corneal endothelial cells is to maintain the stroma in a state of deturgescence using a pump-and-leak mechanism, whilst providing the cornea with nutrients (mostly glucose), from the anterior chamber by passive leakage.[6] As a consequence, the synthetic membranes need to exhibit sufficient diffusion capacities, which was assessed using a glucose diffusion assay in a side- by-side diffusion cell set-up (Figure 4C). The results showed that the PDLLA membranes enable efficient trans-membrane diffusion of glucose (i.e., permeability coefficient of $P_{app} = 1.52 \times 10^{-2} \pm 6.19 \times 10^{-3}$ cm s^{-1}), which can be considered the limiting layer due to the hydrophobicity of the
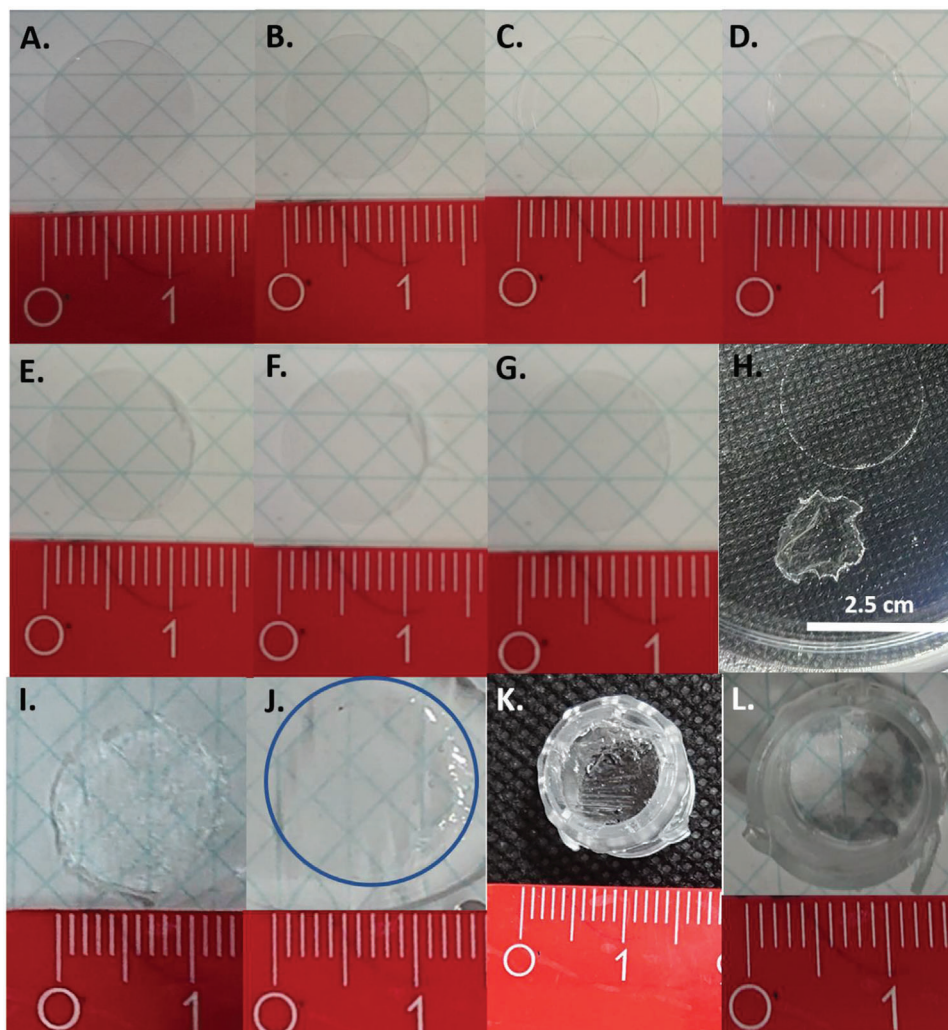
Figure 6. Photographs of the produced membranes: after spin coating on glass slides demonstrating the transparency qualitatively. A) Blank glass; B) glass + gelatin A; C) glass + gelatin A + PDLLA; D) glass + gelatin A + PDLLA + gel-MOD DS 63; E) glass + gelatin A + PDLLA + gel-MOD DS 95; F) glass + gelatin A + PDLLA + gel-MOD-AEMA; G) glass + gelatin A + PDLLA + gel-NB DS 63. H) The isolation of the membrane after dissolving the sacrificial gelatin A. After isolation from the glass slide: I) in the dry state and J) after hydration. K,L) mounted in a CellCrown in a respective dry and hydrated state.

PDLLA. Furthermore, introducing a crosslinked gelatin layer did not lead to any significant differences in permeability between the membranes thereby confirming that the PDLLA layer is indeed the limiting factor (**Table 2** and Figure 4C). When comparing these values to literature, the diffusion still surpasses that of natural Descemet membranes (i.e., 1.2×10^{-5} cm s^{-1}).[29] The obtained permeability coefficients are several orders of magnitude higher than the ones recorded for the natural Descemet membrane (Table 2). We anticipate that higher diffusion values are more desirable than lower diffusion values as this does not preclude the pumping function of the cells, while allowing sufficient transport of nutrients toward the stroma. Furthermore, when combining the permeability coefficients with the measured membrane thicknesses, the diffusion coefficients (D) can be calculated based on Equation (3).[54]

$$D = P_{app} \times T \tag{3}$$

With T being the membrane thickness (cm);

The obtained diffusion coefficients are represented in Table 2. When comparing these values to previously reported values from literature (i.e., $D = 2.55 \times 10^{-7}$ cm^2 s^{-1} for gelatin and atelocollagen membranes) it can be concluded that a similar order of magnitude was obtained.[18]

3.5. In Vitro Biological Assays

3.5.1. Corneal Endothelial Cell Culture

B4G12 immortalized corneal endothelial cells were seeded at a density of 15 000 cells cm^{-2}. Cell attachment to the membranes was observed 4 h after seeding and cells grew to confluency after 1 week of culture on a 12 mm diameter membrane. In every condition, the typical hexagonal morphology of corneal endothelial

ADVANCED
SCIENCE NEWS
www.advancedsciencenews.com

ADVANCED
HEALTHCARE
MATERIALS
www.advhealthmat.de

Table 2. Comparison of the permeability coefficient (P_{app}), membrane thickness, and calculated diffusion coefficients (D) from these values compared to the natural Descemet membrane.

	gel-MOD 95	gel-Mod 63	gel-MOD-AEMA	gel-NB 63	PDLLA	Descemet membrane
P_{app} [cm s^{-1}]	2.36E−02	3.06E−02	9.35E−03	2.55E−02	1.52E−02	1.20E−05[29]
sd	1.90E−02	1.51E−02	8.85E−03	2.47E−02	6.19E−03	
Thickness [nm]	8.58E+02	8.68E+02	7.60E+02	9.08E+02	5.85E+02	1.00E+04[30]
sd	1.82E+02	2.62E+02	3.19E+02	5.69E+02	1.56E+02	
D [cm² s^{-1}]	2.03E−06	1.91E−06	7.10E−07	2.99E−06	8.87E−07	1.20E−08
sd	1.75E−06	1.12E−06	6.72E−07	2.18E−06	3.62E−07	

cells (CEnCs) was preserved. During these experiments, no form of additional coating agent was applied to enable the endothelial cells to adhere to any of the membranes. Corneal endothelial cells are known for their difficulty to expand in vitro with regard to attachment and expansion, which emphasizes the propensity of the modified gelatin derivatives to mimic the extracellular matrix. Alternative approaches to enhance the attachment of cells to tissue culture plastic include the supplementation of ROCK inhibitor in the growth medium and through means of forced attachment with hyaluronic acid.[56,57]

3.5.2. Phenotyping

To date, there is no consensus on the correct markers to demonstrate the phenotypic profile of properly cultured corneal endothelial cells. However, the combination of ZO-1 and Na$^+$/K$^+$ ATPase ion pumps are the most investigated combination of markers reported in literature, to represent the in vivo barrier and pump function of the cell layer, respectively.[58]

In that regard, it is shown that ZO-1 is expressed along the lateral cell membranes of corneal endothelial cells cultured for 1 week on any of the gelatin-polyester combination membranes. Additionally, the staining pattern clearly delineates the hexagonal shape of the cells which is an arbitrary parameter for "healthy" corneal endothelial cells[59] (**Figure 7**). Furthermore, Na$^+$/K$^+$ ATPase are also expressed at the basolateral membranes of the corneal endothelial cells, proving that they still express a high density of ion pumps which is typical for CEnCs. They do not attach well on FNC coated glass cover slips. However, they were included to compare the control condition at the same magnification and resolution, which would not be possible with standard tissue culture plastic as it is too thick for fluorescence microscopy.

It can be observed that the samples with higher crosslink density display a more specific membranous staining pattern than their less crosslinked counterparts. As mentioned before, the Young's modulus of gel-MOD-AEMA approaches that of the Descemet membrane to the greatest extent, which could explain why the phenotype of cells grown on that membrane appears superior to that of less crosslinked membranes.[33]

3.5.3. Adhesion Assay

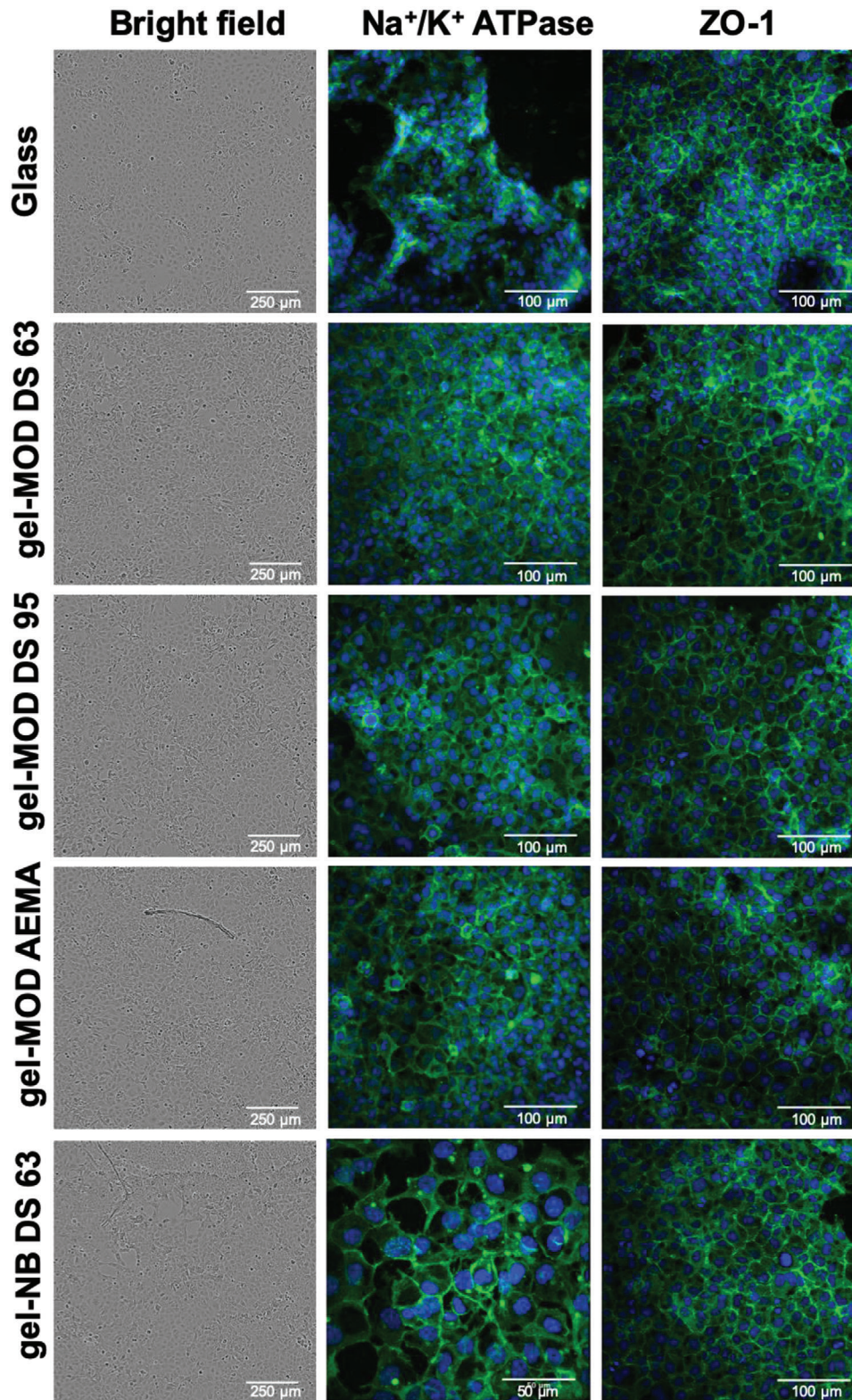To quantify the propensity of cells to initiate adhesion to the candidate scaffold materials, the surface area of focal adhesions per cell was quantified and divided by the surface area of the cell, 24 h after seeding. There was no significant difference in this ratio between the positive control, that is, cell culture plastic coated with the FNC coating mix, the most favorable in vitro growth condition, and the gelatin derivatives in terms of FA/cell surface area ratio. However, when looking to these parameters separately, the cells cultured on plastic displayed both a bigger size of focal adhesions and cell area (**Figure 8**B,C). Previous studies have shown that cell size and the rate of enlargement is higher with increased substrate stiffness.[60,61] This phenomenon can explain the larger size of cells grown on TCP, which has a Young's modulus around 100 000 kPa. However, a similar FA area to cell size ratio on both plastic and gelatins indicates that within the first 24 h, the cells are equally able to develop focal adhesions upon being seeded on tissue culture plastic and on the gelatin derivatives.

3.5.4. Proliferation Assay

From exponential growth curves, PDT were calculated to compare the growth rate on the different scaffolds (**Figure 9**). From that analysis, there was no significant different between the cells grown on gelatin scaffolds (range: 44–58 h) or the positive control (35.84 ± 0.97 h), that is, tissue culture plastic coated with FNC coating mix. However, the corneal endothelial cells that grew on coated glass cover slips had a significantly higher PDT compared to coated tissue culture plastic, as the high stiffness of glass creates an inhospitable environment for cell homeostasis. To conclude, every type of gelatin scaffold is able to sustain cell growth to the same degree as the coated culture plastic benchmark, thereby proving its cytocompatible features in vitro.

3.5.5. Primary Corneal Endothelial Cell Culture

Primary corneal endothelial cells were cultivated on gel-MOD-AEMA as a proof-of-concept for these membranes as an endothelial scaffold. Cells were grown for 1 week on these scaffolds without an additional FNC coating and stained for their Na$^+$/K$^+$ ATPase ion pumps and ZO-1 expression (**Figure 10**). Both proteins were expressed at the basolateral membrane and the cells displayed a hexagonal morphology, proving the suitability of the developed membranes toward primary corneal endothelial cells.

ADVANCED
SCIENCE NEWS

www.advancedsciencenews.com

ADVANCED
HEALTHCARE
MATERIALS

www.advhealthmat.de

Figure 7. Morphology and phenotype of cells grown on gelatin derivatives. Left column lists phase contrast images taken at 10× magnification. Middle and right column are fluorescent images of cells grown on gelatin derivatives and were stained for Na$^+$/K$^+$ ATPase and ZO-1 respectively. Note that the gel-NB DS63 was taken on a 40× magnification whereas the other images were recorded at 20× magnification.
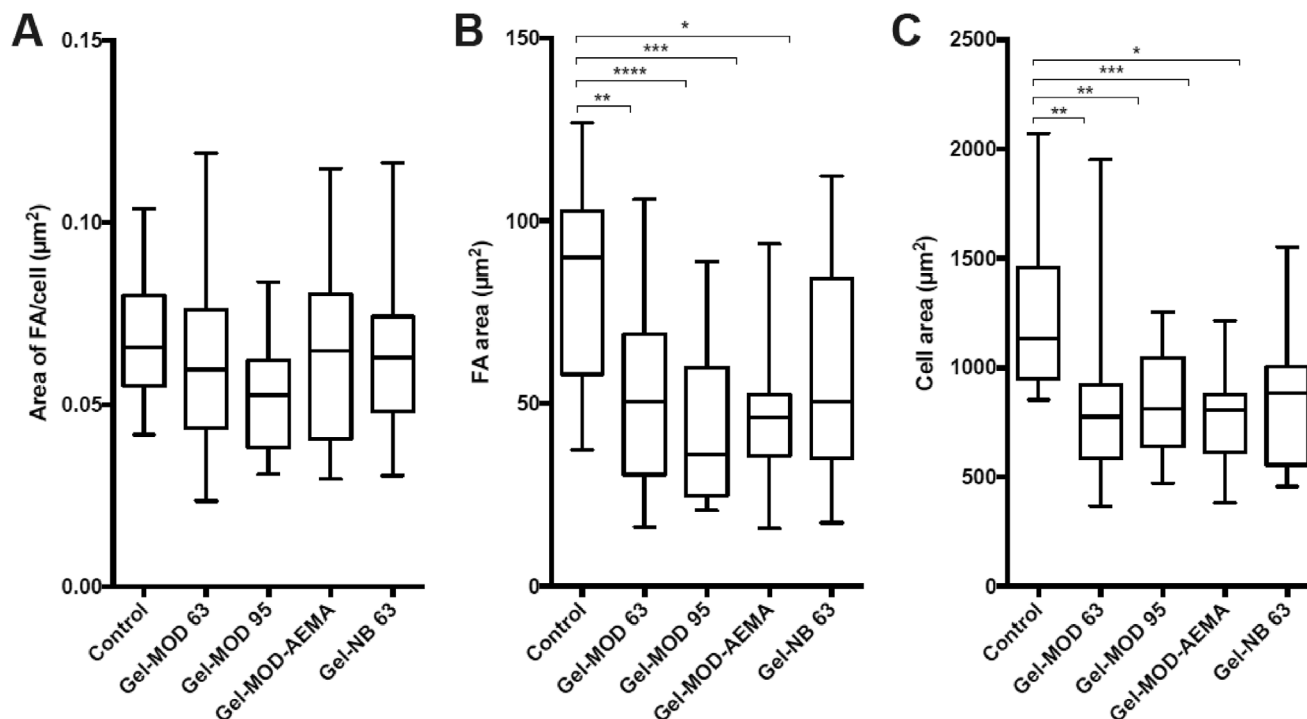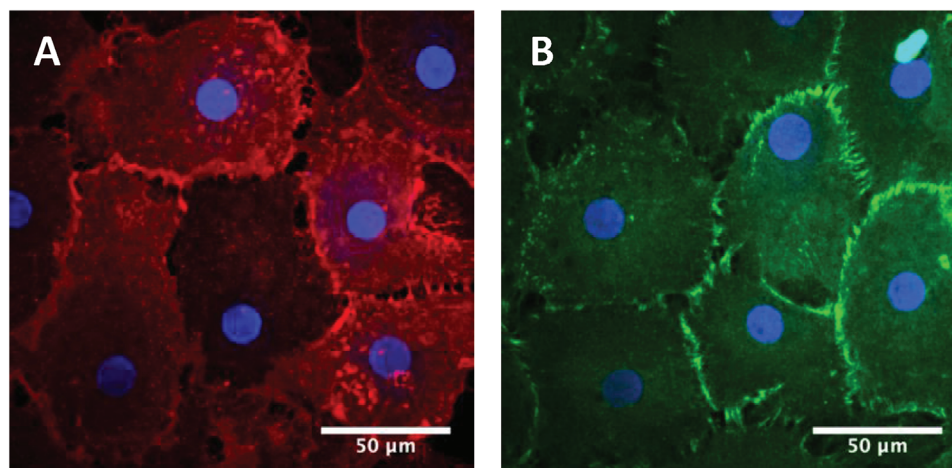
Figure 8. Graphical representation of A) the ratio of the focal adhesion area of a cell divided by the cell surface area, B) the focal adhesion area per cell, and C) the cell surface area.
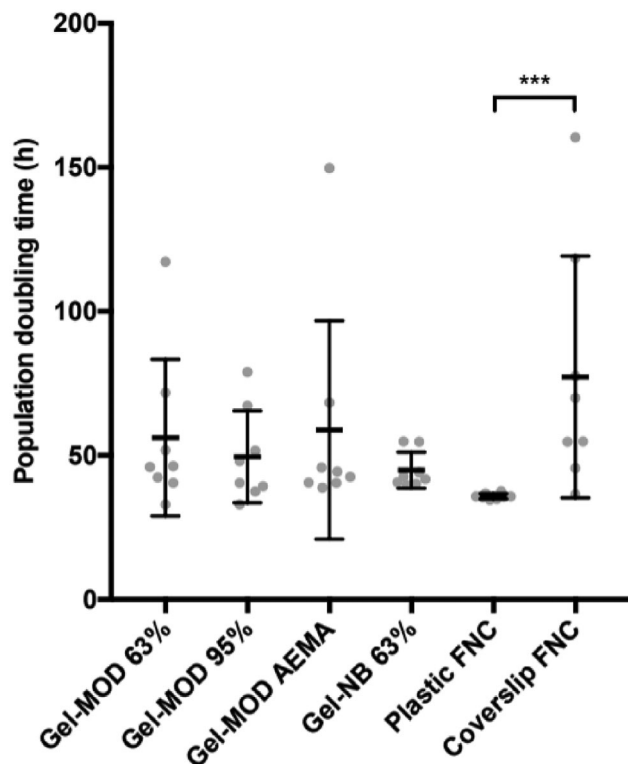
Figure 9. Population doubling times of CEnC grown on modified gelatin. There was no significant different between the positive control (plastic FNC) and the crosslinked gelatins. CenC did grown slower on a glass coverslip coated with FNC.

4. Conclusion

This study demonstrates the potential of applying PDLLA-gelatin multilayer membranes for corneal endothelial tissue engineering. This strategy resulted in ultrathin membranes (i.e., <1 µm) that benefit both from a comparable mechanical strength as the natural membranes (±5 MPa) due to the presence of the PDLLA and the ECM mimicking capacity of the gelatin derivatives. These materials prove very suitable for the application as every gelatin derivative will be hydrolyzed and broken down into peptides in vivo, similarly to collagen breakdown in the human body. The PDLLA supporting polymer, will be degraded to lactic acid, which should not pose any problems in the corneal environment as 85% of glucose in the cornea is metabolized into lactate which is even considered as a contributing anion flux to maintain corneal transparency. Although, the gelatin coatings have proven to be a very suitable ECM mimic in the present application, the experiments do not further reveal an outperforming candidate among the different modified gelatins both in terms of physico-chemical and biological performance. However, the samples with the highest Young's modulus, namely gel-MOD DS 95, and gel-MOD-AEMA, are considered to be a better mimic of the Descemet membrane, due to a closer match to the native membrane in terms of mechanical properties. Therefore, for future studies, the choice for a suitable gelatin derivative can be made based on most straightforward membrane fabrication. As a result, the most promising candidate gelatin derivative would be gel-MOD-AEMA due to the following reasons. First, gel-MOD-AEMA displays a higher Young's modulus which is a closer match to the in vivo value of the Descemet membrane. Second, due to its higher

**ADVANCED
SCIENCE NEWS**

www.advancedsciencenews.com

**ADVANCED
HEALTHCARE
MATERIALS**

www.advhealthmat.de

Figure 10. Primary corneal endothelial cells cultivated on gel-MOD-AEMA and stained for their respective A) ZO-1 and B) Na^+/K^+ ATPase ion pumps (40× magnification).

degree of crosslinking, it is expected to swell less in vivo and degrade at a slower rate which is beneficial as corneal endothelial cells secrete only very limited extracellular matrix through life, making a slowly degrading ECM mimicking material more interesting. Third, gel-MOD-AEMA can easily be processed at room temperature in contrast to the other assessed gelatin derivatives. Furthermore, in contrast to the step-growth based norbornene derivatives, processing of a chain growth derivative (i.e., gel-MOD and gel-MOD-AEMA) can occur in a straightforward manner since there are no issues related to thiol stability at the required elevated temperatures to keep gelatin in solution or preliminary crosslinking due to the high reactivity. As a proof-of-concept experiment, the gel-MOD-AEMA membranes were also used to culture primary corneal endothelial cells, which exhibited the desirable hexagonal morphology, Na^+/K^+ ATPase ion pumps and ZO-1 protein expression. Through this innovative combination of PDLLA with gelatin, we have managed to incorporate the mechanical strength of the polyester and the ECM-mimicking capacity of gelatin in an ultra-thin scaffold for corneal endothelial transplantation.

Supporting Information

Supporting Information is available from the Wiley Online Library or from the author.

Conflict of Interest

At the start of this work a couple of years ago, N.Z. was employed by the University of Antwerp. Meanwhile, she is employed by Novartis, but also is still affiliated with the University of Antwerp.

[1] WHO, Priority Eye Diseases, http://www.who.int/blindness/causes/priority/en/index9.html (accessed: June 2020).

[2] J. P. Whitcher, M. Srinivasan, M. P. Upadhyay, *Bull. W. H. O.* **2001**, *79*, 214.

[3] E. Flockerzi, P. Maier, D. Böhringer, H. Reinshagen, F. Kruse, C. Cursiefen, T. Reinhard, G. Geerling, N. Torun, B. Seitz, *Am. J. Ophthalmol.* **2018**, *188*, 91.

[4] G. Bigan, M. Puyraveau, M. Saleh, P. Gain, I. Martinache, B. Delbosc, A. S. Gauthier, *Eur. J. Ophthalmol.* **2018**, *28*, 535.

[5] *2016 Eye Banking Statistical Report*, Eye Bank Association of America, Washington, DC **2017**.

[6] B. van den Bogerd, S. N. Dhubhghaill, C. Koppen, M. J. Tassignon, N. Zakaria, *Surv. Ophthalmol.* **2018**, *63*, 149.

[7] M. O. Price, P. Gupta, J. Lass, F. W. Price, *Ann. Rev. Vision Sci.* **2017**, *3*, 69.

[8] P. Gain, R. Jullienne, Z. He, *JAMA Ophthalmol.* **2016**, *134*, 167.

[9] S. Kinoshita, N. Koizumi, M. Ueno, N. Okumura, K. Imai, H. Tanaka, Y. Yamamoto, T. Nakamura, T. Inatomi, J. Bush, M. Toda, M. Hagiya, I. Yokota, S. Teramukai, C. Sotozono, J. Hamuro, *N. Engl. J. Med.* **2018**, *378*, 995.

[10] B. van den Bogerd, S. Ní Dhubhghaill, N. Zakaria, *J. Tissue Eng. Regener. Med.* **2018**, *12*, 2020.

[11] J. Navaratnam, T. P. Utheim, V. K. Rajasekhar, A. Shahdadfar, *J. Funct. Biomater.* **2015**, *6*, 917.

[12] J. van Hoorick, L. Tytgat, A. Dobos, H. Ottevaere, J. van Erps, H. Thienpont, A. Ovsianikov, P. Dubruel, S. van Vlierberghe, *Acta Biomater.* **2019**, *97*, 46.

[13] R. Schrieber, H. Gareis, *Gelatine Handbook: Theory and Industrial Practice*, Wiley, Weinheim **2007**.

[14] I. van Nieuwenhove, A. Salamon, K. Peters, G. Graulus, J. C. Martins, D. Frankel, K. Kersemans, F. de Vos, S. van Vlierberghe, P. Dubruel, *Carbohydr. Polym.* **2016**, *152*, 129.

**ADVANCED
SCIENCE NEWS**

www.advancedsciencenews.com

**ADVANCED
HEALTHCARE
MATERIALS**

www.advhealthmat.de

[15] J. van Hoorick, P. Gruber, M. Markovic, M. Tromayer, J. van Erps, H. Thienpont, R. Liska, A. Ovsianikov, P. Dubruel, S. van Vlierberghe, *Biomacromolecules* **2017**, *18*, 3260.

[16] A. I. van den Bulcke, B. Bogdanov, N. de Rooze, E. H. Schacht, M. Cornelissen, H. Berghmans, *Biomacromolecules* **2000**, *1*, 31.

[17] B. J. Klotz, D. Gawlitta, A. J. W. P. Rosenberg, J. Malda, F. P. W. Melchels, *Trends Biotechnol.* **2016**, *34*, 394.

[18] R. Watanabe, R. Hayashi, Y. Kimura, Y. Tanaka, T. Kageyama, S. Hara, Y. Tabata, K. Nishida, *Tissue Eng., Part A* **2011**, *17*, 2213.

[19] M. Rizwan, G. S. L. Peh, H. P. Ang, N. C. Lwin, K. Adnan, J. S. Mehta, W. S. Tan, E. K. F. Yim, *Biomaterials* **2017**, *120*, 139.

[20] S. van Vlierberghe, B. Fritzinger, J. C. Martins, P. Dubruel, *Appl. Spectrosc.* **2010**, *64*, 1176.

[21] J. van Hoorick, P. Gruber, M. Markovic, M. Rollot, G. J. Graulus, M. Vagenende, M. Tromayer, J. van Erps, H. Thienpont, J. C. Martins, S. Baudis, A. Ovsianikov, P. Dubruel, S. Van Vlierberghe, *Macromol. Rapid Commun.* **2018**, *39*, e1800181.

[22] J. van Hoorick, L. Tytgat, A. Dobos, H. Ottevaere, J. van Erps, H. Thienpont, A. Ovsianikov, P. Dubruel, S. van Vlierberghe, *Acta Biomater.* **2019**, *97*, 46.

[23] K. E. Pfitzner, J. G. Moffatt, *J. Am. Chem. Soc.* **1963**, *85*, 3027.

[24] M. Save, A. Soum, *Macromol. Chem. Phys.* **2002**, *203*, 2591.

[25] Corbion, Biomedical Materials that Make a Difference, https://www.corbion.com/biomaterials (accessed: May 2020).

[26] U.S. Food & Drug Administration (FDA), List of Drug Master Files (DMFs), https://www.fda.gov/drugs/drug-master-files-dmfs/list-drug-master-files-dmfs (accessed: **2020**).

[27] T. Desmet, T. Billiet, E. Berneel, R. Cornelissen, D. Schaubroeck, E. Schacht, P. Dubruel, *Macromol. Biosci.* **2010**, *10*, 1484.

[28] E. de Jaeghere, E. de Vlieghere, J. van Hoorick, S. van Vlierberghe, G. Wagemans, L. Pieters, E. Melsens, M. Praet, J. van Dorpe, M. N. Boone, R. Ghobeira, N. De Geyter, M. Bracke, C. Vanhove, S. Neyt, G. Berx, B. G. De Geest, P. Dubruel, H. Declercq, W. Ceelen, O. De Wever, *Biomaterials* **2018**, *158*, 95.

[29] J. H. Kim, K. Green, M. Martinez, D. Paton, *Exp. Eye Res.* **1971**, *12*, 231.

[30] J. Teichmann, M. Valtink, M. Nitschke, S. Gramm, R. H. W. Funk, K. Engelmann, C. Werner, *J. Funct. Biomater.* **2013**, *4*, 178.

[31] M. Markovic, J. van Hoorick, K. Hölzl, M. Tromayer, P. Gruber, S. Nürnberger, P. Dubruel, S. van Vlierberghe, R. Liska, A. Ovsianikov, *J. Nanotechnol. Eng. Med.* **2015**, *6*, 021004.

[32] M. Parekh, B. van den Bogerd, N. Zakaria, D. Ponzin, S. Ferrari, *Stem Cells Int.* **2018**, *2018*, 8146834.

[33] R. N. Palchesko, K. L. Lathrop, J. L. Funderburgh, A. W. Feinberg, *Sci. Rep.* **2015**, *5*, 7955.

[34] J. A. Last, S. J. Liliensiek, P. F. Nealey, C. J. Murphy, *J. Struct. Biol.* **2009**, *167*, 19.

[35] T. K. L. Meyvis, B. G. Stubbe, M. J. van Steenbergen, W. E. Hennink, S. C. de Smedt, J. Demeester, *Int. J. Pharm.* **2002**, *244*, 163.

[36] C. W. Macosko, *Rheology: Principles, Measurements, and Application*, Wiley, Weinheim **1994**. ISBN: 978-0-471-18575-8.

[37] C. E. Hoyle, C. N. Bowman, *Angew. Chem., Int. Ed.* **2010**, *49*, 1540.

[38] J. D. McCall, K. S. Anseth, *Biomacromolecules* **2012**, *13*, 2410.

[39] C. E. Hoyle, T. Y. Lee, T. Roper, *J. Polym. Sci., Part A: Polym. Chem.* **2004**, *42*, 5301.

[40] A. Dobos, J. van Hoorick, W. Steiger, P. Gruber, M. Markovic, O. G. Andriotis, A. Rohatschek, P. Dubruel, P. J. Thurner, S. van Vlierberghe, S. Baudis, A. Ovsianikov, *Adv. Healthcare Mater.* **2019**, 1900752.

[41] Y. Wang, W. Qu, S. H. Choi, *Am. Pharm. Rev.* **2016**, *19*, 188841.

[42] U.S. Food and Drug Administration (FDA), U.S Department of Health and Human Services **2018**, *3*.

[43] U.S. Department of Health and Human Services, **2016**, 1.

[44] G. Graulus, N. van Herck, K. van Hecke, G. van Driessche, B. Devreese, H. Thienpont, H. Ottevaere, S. van Vlierberghe, P. Dubruel, *React. Funct. Polym.* **2018**, *128*, 16.

[45] A. Gierej, M. Vagenende, A. Filipkowski, B. Siwicki, R. Buczynski, H. Thienpont, S. van Vlierberghe, T. Geernaert, P. Dubruel, F. Berghmans, *J. Lightwave Technol.* **2019**, *37*, 1916.

[46] J. A. Bonanno, *Exp. Eye Res.* **2012**, *95*, 2.

[47] S. Matthyssen, B. van den Bogerd, S. Ni Dhubhghaill, C. Koppen, N. Zakaria, in *Stem Cells in Clinical Applications*, (Ed: P. V. Pham), Springer, Berlin **2016**, pp. 213–255.

[48] L. Tytgat, L. van Damme, J. van Hoorick, H. Declercq, H. Thienpont, H. Ottevaere, P. Blondeel, P. Dubruel, S. van Vlierberghe, *Acta Biomater.* **2019**, *94*, 340.

[49] E. Hoch, T. Hirth, G. E. M. Tovar, K. Borchers, *J. Mater. Chem. B* **2013**, *1*, 5675.

[50] F. A. Guarnieri, *Corneal Biomechanics and Refractive Surgery*, Springer, Berlin **2015**.

[51] Q. Shi, Q. Fan, W. Ye, J. Hou, S. C. Wong, X. Xu, J. Yin, *ACS Appl. Mater. Interfaces* **2014**, *6*, 9808.

[52] C. C. Danielsen, *Exp. Eye Res.* **2004**, *79*, 343.

[53] M. M. Jumblatt, D. M. Maurice, B. D. Schwartz, *Transplantation* **1980**, *29*, 498.

[54] G. Niu, J. S. Choi, Z. Wang, A. Skardal, M. Giegengack, S. Soker, *Biomaterials* **2014**, *35*, 4005.

[55] K. H. Kurji, A. Y. Cheung, M. Eslani, E. J. Rolfes, D. Y. Chachare, N. J. Auteri, M. L. Nordlund, E. J. Holland, *Cornea* **2018**, *37*, 1226.

[56] M. Parekh, S. Ahmad, A. Ruzza, S. Ferrari, *Sci. Rep.* **2017**, *7*, 142.

[57] N. Okumura, R. Inoue, Y. Okazaki, S. Nakano, H. Nakagawa, S. Kinoshita, N. Koizumi, *Invest. Ophthalmol. Visual Sci.* **2015**, *56*, 6067.

[58] B. van den Bogerd, N. Zakaria, B. Adam, S. Matthyssen, C. Koppen, S. N. Dhubhghaill, *Transl. Vision Sci. Technol.* **2019**, *8*, 13.

[59] G. S. L. Peh, K.-P. Toh, H.-P. Ang, X.-Y. Seah, B. L. George, J. S. Mehta, *BMC Res. Notes* **2013**, *6*, 176.

[60] T. Yeung, P. C. Georges, L. A. Flanagan, B. Marg, M. Ortiz, M. Funaki, N. Zahir, W. Ming, V. Weaver, P. A. Janmey, *Cell Motil. Cytoskeleton* **2005**, *60*, 24.

[61] A. Skardal, D. Mack, A. Atala, S. Sokern, *J. Mech. Behav. Biomed. Mater.* **2012**, *17*, 307.